

Modeling of a Rope-Free Passenger Transportation System with Closed Kinematic Chain

Jonas Missler* Markus Jetter** Oliver Sawodny*

* Institute for System Dynamics, University of Stuttgart
Waldburgstrasse 19, 70563 Stuttgart, Germany
(e-mail: {missler,sawodny}@isys.uni-stuttgart.de).

** thyssenkrupp Elevator AG, Test Tower Rottweil, Berner Feld 60,
78628 Rottweil, Germany (e-mail: markus.jetter@thyssenkrupp.com)

Abstract: Passenger comfort is one of the main concerns in the acceptance of a new passenger transportation system (PTS). Especially in vertical transportation systems, classically realized by cable elevators, the highest possible ride quality is expected by the market. In the rope-free PTS the rope of the standard elevator is replaced by a linear motor, which directly provides the driving force. The new propulsion and in particular the possibility of horizontal movement inside the shaft, demands a new design of the vehicle. This paper will present a model of the PTS with the focus on passenger comfort and therefore on the aspect of active vibration damping. The presented model also includes an actuator model of the damping components, which form with a closed kinematic chain together with the PTS. Measurements on the real MULTI test system of the novel PTS, which is installed in the test tower in Rottweil, Germany, are used to identify the model parameters.

Keywords: Mechatronic systems, Modeling, Mechatronics for Mobility Systems, Identification, Ride Comfort

1. INTRODUCTION

Vertical passenger transportation in buildings has been carried out for decades with classical cable elevators. The highest elevator is currently installed in the Shanghai Tower in Shanghai with a height of 578 meters. The achieved travel height in what is currently the tallest skyscraper is an achievement in itself, but also poses the greatest challenge of classical cable elevators: the rope. At travel heights over 300 meters not only the weight of the rope starts to become a problem, but also the rope sway inside the elevator shafts. In the case of an external excitation of the building, e.g. by wind, the elevator rope inside the shaft is also excited, which can cause the ropes to hit the shaft walls. If rope sway is present, the elevator can often still be operated at reduced velocity; under more extreme conditions, passenger elevators may have to be stopped. Naturally, this problem increases with the height of buildings, and every reduction of travel velocity goes along with a reduction in handling capacity of the elevator. Rope sway in high buildings is the main reason for the desire to design a vertical passenger transportation system (PTS), which does not rely on ropes.

Conventional rope elevators use a rotatory torque generated by an electric motor at the top of the shaft, which is conveyed via ropes to a vertical force on the elevator car. The MULTI by thyssenkrupp replaces the propulsion system by a linear motor, thus the electromagnetic vertical force is directly generated at the current location of the car in the shaft. At the test tower in Rottweil, Germany,

the first full-scale MULTI test system of a rope-free PTS has been implemented, its propulsion is an ironless long-stator linear synchronous motor, see Appunn et al. (2018). The general structure of the rope-free PTS is displayed in Figure 1.

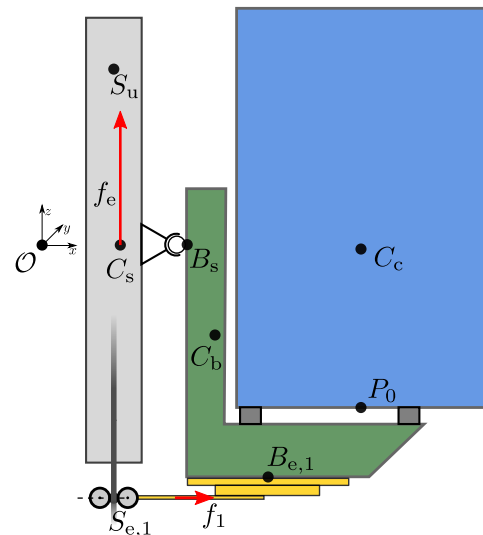


Fig. 1. Principle sketch of the rope-free passenger transportation system.

In passenger transportation the linear motor is mainly used for horizontal transport, e.g. in the Transrapid Maglev System, see Heinrich and Kretzschmar (1989). While

there exist many ideas to use the linear motor inside an elevator, the first concepts replaced the rotatory drive with a linear drive but still kept the rope, see DE2002081 (A1). Karl Kudermann. (1970), the MULTI test system in Rottweil is the first full-scale vertical PTS. The complete bypass of the rope leads to additional advantages compared to standard rope elevators, beside the theoretical infinite extension in travel height. Changing the propulsion also leads to the possibility of multiple cabins in the same shaft, which can ride in a row after each other. In addition, the linear motor is not restricted to vertical travel, but enables horizontal travel of the PTS. The combination of multiple cars and horizontal movement enables in the simplest stage a modern version of the Paternoster, a non-stop elevator that moves in a loop inside two shafts and was developed as *Cyclic Lift* by Peter Hart in 1882. At the test tower in Rottweil a new interpretation of this Paternoster is possible. Two shafts are fitted with two parallel PTS tracks and the cars can exchange shafts at the top and half height of the tracks.

One of the main points in the acceptance of a new transportation system, especially in vertical transportation, is the ride quality of the system. The aim for the rope-free PTS is to reach at least the same ride quality standards as cable elevators. This paper focuses on the modeling of the MULTI test system of the rope-free PTS with regard to active vibration damping for passenger comfort. The model is generated as a Multi-Body System (MBS), Bottasso (2009), taking advantage of the basic structure of the MULTI test system, which is displayed in Figure 1. In addition, an actuator model of the active damping components underneath the mounting frame is given. The combination of actuator and PTS form a closed kinematic chain via the guidance rails, which requires additional modeling presented here. The mechanical model is split up into a part of the known dynamic and an unknown disturbance part. The disturbance part of the model is used to bypass the necessity to perfectly model all disturbances. More precisely, the problem being addressed is the damping of vibrations inside the cabin and therefore, the motion of the sledge is viewed as the disturbance dynamics to the system. The sledge sits at the back of the shaft and holds the permanent magnets of the linear motor. A planar model variant of the MULTI test system was derived in Missler et al. (2016). In contrast to that paper, the here presented model is a three-dimensional and the location of the damping actuators changed. Furthermore, the sledge is not neglected in the present model.

The structure of the paper is as follows, the first section summarizes the PTS structure and states the basic performance values to rate the ride comfort of elevators. The second section describes the mechanical model of the PTS and the actuator model of the damping components. The given linearization of the mechanical model is used for the identification of the stiffness and damping parameters. Before the conclusion simulations of the resulting model will be compared with measurements performed at the test tower in Rottweil.

2. ROPE-FREE VERTICAL PASSENGER TRANSPORTATION SYSTEM

The propulsion of the rope-free PTS is moved from the top of the elevator shaft to the back of the shaft. The active components of the linear motor are directly mounted on the back of the elevator shaft and the passive elements, thus the permanent magnets, are at the back of the elevator car. Beside containing the passive part of the linear motor, the so-called sledge carries the guide rollers, which hold the sledge in place and ensure a tight air gap for the linear motor. The second part of the PTS is the mounting frame, whose main task is the support of the cabin from below. It is shaped as an 'L', see Figure 1, with two forks underneath the cabin. At the connection point B_s to the sledge is a bearing, which is locked during rides and can rotate passively in case the PTS moves horizontally, thus the cabin keeps its orientation and only the sledge is rotated 90 degrees. Further, the cabin is connected to the mounting frame via four passive dampers, so that the mounting frame supports the cabin from below. The third body is the cabin, which like in any other elevator will carry the passengers. Sledge, mounting frame and cabin form the elevator car. The cabin is for the measurements replaced by a wooden plate, in order to carry the measurement and control equipment on the MULTI test system. In order to be able to actively damp the cabin in the horizontal plane, underneath both forks of the mounting frame additional active components were fitted. The basic idea of this damping components is to mitigate vibrations in rotatory motion around the bearing. The sketch in Figure 1 shows one one actuator at the bottom of the mounting frame, which applies the force f_1 .

In addition to the existing position measurement, necessary for the propulsion system, the MULTI test system in Rottweil is equipped with two Inertial Measurement Units (IMUs). The first IMU is used to measure the vibrations inside the cabin and is therefore placed in the center of the cabin floor at point P_0 . The second IMU is used to measure the disturbances directly at the sledge. It is located at the point S_u at the top of the sledge close to the upper guidance rollers, see Figure 1 for the points P_0 and S_u .

One requirement of the MULTI test system was the best possible efficiency of the propulsion system, so the aim was to keep the air gap as close as possible to its optimum value. Therefore, a very stiff connection to the guidance rails is required and the stiffness and damping of the guidance rollers was chosen accordingly. The disadvantage of the stiff connection from the car to the guidance is that every small unevenness from the rail is conveyed directly to the cabin. Also the possibility of horizontal travel with the MULTI test system demands a so-called back-pack suspension, which is not ideal in the sense of passenger comfort. Commonly ropes of standard elevators are attached in the center of the cabin, therefore the torques caused by the traction force are kept at a minimum. Moreover, a frame around the cabin contains additional passive damping elements, which help decouple the cabin from the shaft, and improve the ride comfort of standard elevators. For the back-pack solution of the PTS on the other hand the traction force is applied

at the back and therefore causes significant torques in the acceleration phase. In addition, the linear motor and especially the missing counterweight demands a light-weight construction for the car, because the whole car weight has to be accelerated during the ride. All these measures have a great influence on the vibrations inside the cabin and therefore on the ride comfort during an elevator ride.

Ride comfort in the elevator environment is evaluated using the norm ISO18738-1:2012 (2012), which describes in detail every aspect of passenger comfort during an elevator ride. Mechanical vibrations felt inside the cabin are the main focus of this work and therefore only the calculation of the peak-to-peak vibration values are of interest. The calculation of these peak-to-peak values is based on acceleration measurements taken during an elevator ride, where the sensor was placed in the middle of the cabin floor. The principle approach of the calculation is first the weighting of the acceleration measurement according to the human sensitivity. The weighting is analog to ISO2631-1:1997 (1997) and is given in Figure 2. Vibrations in the vertical travel direction, thus z -direction, are felt differently than the vibration along the horizontal x - y -plane perpendicular to the travel direction. A different weighting function is used for horizontal and vertical vibrations. The second step is the calculation of the peak-to-peak values of these weighted accelerations. In the last step the A95-peak-to-peak is calculated, which is the highest peak-to-peak value after five percent of the largest peak-to-peak values are ignored. This A95 value is the main value used to compare ride comfort with regard to mechanical vibrations.

Explicit values, which ensure a pleasant ride are not given in the standard ISO18738-1:2012 (2012). The VDI guideline VDI2057 (2015) places the perception threshold for vibrations at 0.015 m/s^2 for the effective acceleration value. The aim for the PTS has to be at least the lower end of the barely perceptible region, which lies between 0.02 and 0.8 m/s^2 , in order to meet and exceed market standards. The acceleration thresholds in the VDI guideline are defined for Root Mean Square (RMS) values, correspondingly, a typical factor of eight between noise and peak-to-peak is used to get the peak-to-peak performance values and four as the RMS to A95 factor. In summary, the standard ISO18738-1:2012 (2012) states algorithms for the calculation of performance values, which are used to compare different elevators with each other.

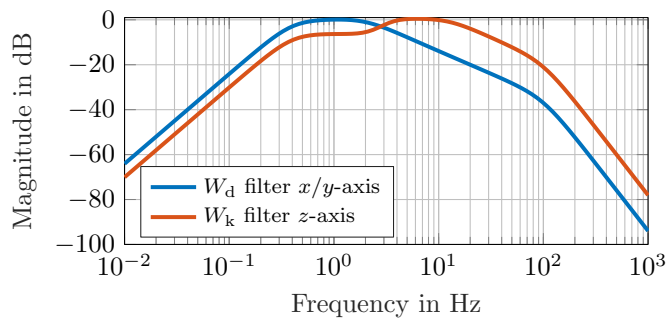


Fig. 2. Frequency weighting by human sensitivity according to standard ISO2631-1:1997 (1997).

3. MODEL OF THE PASSENGER TRANSPORTATION SYSTEM

The model is separated into the mechanical, thus the PTS car, and the electrical part, which is the electrical dynamics of the damping actuator. The propulsion of the PTS is ignored, because the model focuses on the analysis and active compensation of the vibrations inside the cabin. The mechanical model is derived as rigid MBS and the electrical part is based on the standard permanent linear motor equations. In addition, the MBS contains a closed kinematic chain via the two damping actuators.

3.1 Mechanical Model

The aim of the mechanical model is to depict the three main natural frequencies of the PTS. Basis of the mechanical model is the assumption, that the springs and dampers are concentrated at the bearing B_s between the mounting frame and the sledge. This assumption is based on previous modal analysis of the MULTI test system, the three lowest harmonics of the PTS are all rotations, which rotate close to the bearing point B_s . The coordinate system of the model is as follows, the x -axis points towards the door, thus to the right in Figure 1, the z -axis points in the vertical upwards travel direction, and the y -axis completes the coordinate system to a right-handed coordinate system. The corresponding rotation around the axis are α around the x -axis, β around the y -axis and γ around the z -axis. In summary, the three natural frequencies are represented by three torsional spring and damper pairs at bearing B_s , which are oriented around the x , y and the z -axis respectively.

Model Structure The bodies of the rigid MBS are based on the given structure of the PTS, thus the sledge, the mounting frame and the cabin. Further, mounting frame and cabin are treated as a single body, and the cabin was replaced by a plate, similar to the wooden plate at the MULTI test system, since it was not possible to fix and secure the measurement equipment inside the cabin. In addition, each of the actuators is modeled by two rigid bodies, which results in a total of six rigid bodies.

First the sledge is modeled as a free body in space and has therefore six Degree Of Freedoms (DOFs). It is hold in position by the guidance system, which restrains the motion of the PTSs in all direction except the desired travel direction. The guidance system consists of the guide rails mounted along the shaft and the guide rollers at the sledge. These roller coating works as spring/damper element keeping the sledge in position. The second body of the model is the combination of mounting frame and cabin, which is connected through the bearing at point B_s and has three DOF according to the natural frequencies, that are mapped by the model. The damping actuators are modeled by two bodies each, these are the upper passive part and the lower active part of each linear motor. Each linear motor is mounted underneath the mounting frame and connected via the point B_{ei} to the frame. The lower part is connected to the guidance rail via an extra guidance roller pair at point S_{ei} , with the actuator index $i = 1, 2$. Each actuator has three DOFs, first the actuator position l_i , the other two describe its orientation by two angles

around the point B_{ei} with the rotation around the y -axes by β_i and z -axes by γ_i .

Closed Kinematic Chain The actuators form a closed kinematic chain together with the guide rail, sledge and mounting frame, see Figure 3 for the closing condition of the i -th actuator. The closing condition for one actuator is given by

$$c_i(q^b) = [r_{Si}^O(q^b) + r_{Bei}^{Si}(q^b) - r_{Bs}^O(q^b) - r_{Bei}^{Bs}(q^b)], \quad (1)$$

where the vector $r_{Si}^O + r_{Bei}^{Si}$ is the path from the origin O to the point B_{ei} via the damping actuator and the vector $r_{Bs}^O + r_{Bei}^{Bs}$ describes the path from the origin to the point B_{ei} via sledge and mounting frame, with $i = 1, 2$. In summary, the open kinematic chain MBS has $f^b = 15$ DOFs and with closed kinematic chain the DOFs are reduced to $f = 9$, where the generalized coordinates of the linear motor are neglected.

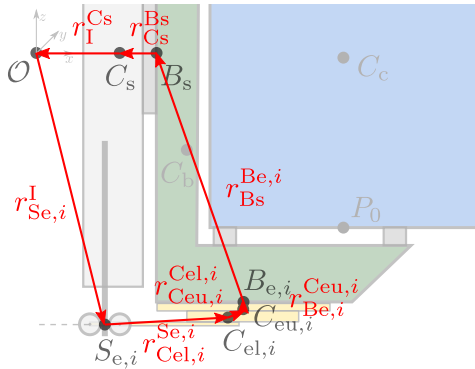


Fig. 3. Closing condition of the MBS for the i -th actuator.

The vector of the generalized coordinates of the open loop are

$$q^b(t) = [x_s, y_s, z_s, \alpha_s, \beta_s, \gamma_s, \alpha_b, \beta_b, \gamma_b, \dots, l_1, \beta_1, \gamma_1, l_2, \beta_2, \gamma_2]^T, \quad (2)$$

where the subscript 's' refers to the six sledge coordinates, the subscript 'b' to the three DOFs at bearing B_s , and the last six are the coordinates of the damping actuators.

Equations of Motion The equations of motion are derived using the Newton-Euler method for each body depending on the generalized coordinates (2). The dynamic equations are all derived in the Center of Gravity (COG) of the respective body. The contact points of each force and joints are described in relation to these COGs of the bodies. On the mounting frame this points are $B_{e,1}$ and $B_{e,2}$. The contact point between actuator and guide rail are at $S_{e,1}$ and $S_{e,2}$. The joint between sledge and mounting frame is at the bearing B_s . Combining all this, the equations of motion for the closed loop model can be formulated in the standard form

$$M(q^b) \ddot{q}(t) = g(q^b, \dot{q}^b) + k(q^b, \dot{q}^b, u(t)), \quad (3)$$

where $q = [x_s, y_s, z_s, \alpha_s, \beta_s, \gamma_s, \alpha_b, \beta_b, \gamma_b]^T$ are six free motions of the sledge and three rotations around the connection point B_s , and the generalized coordinates of the open MBS q^b is given in (2). The input u of the model are both forces of the damping actuators, thus f_1 and f_2 . The initial conditions of the system (3) are $q(0) = q_0 \in \mathbb{R}$, $\dot{q}(0) = \dot{q}_0 \in \mathbb{R}$.

In the form (3), the constraint forces between the bodies of the MBS are eliminated and the dynamic of the MBS is described by a minimal set of independent generalized coordinates q . The dependent coordinates, thus in the present case the coordinates of the actuators, can be calculated via the inverse kinematics based on the closing condition (1). The matrix $M(q^b, t)$ is the symmetric $f \times f$ -inertia matrix, which contains the moments of inertia and masses of the bodies of the MBS. The vector k of the size $f \times 1$ inherits the generalized Coriolis forces as well as elastic and damping forces. The $f \times 1$ -vector g are the generalized applied forces, which contain the external forces acting on the MBS, like the gravitational force. The scalar t represents the time, and was omitted in generalized coordinates q respectively q^b , due to the lack of space.

The model (3) also contains the dynamic of the sledge, which is only described briefly here. The sledge is modeled as a free body with six DOFs, which is connected via six translational spring/damper elements to the guidance system. Four of the spring/damper elements are in the x - z -plane, basically placed in all four corners of the sledge cuboid. Therefore, they constrain the translational motion in x direction and the rotational motion around y and z -axis. The rest of the two spring/damper elements are placed at the top and bottom of the sledge cuboid parallel to the y - z -plane. The second spring/damper pair restricts translational motion in y direction and rotational motion around the x -axis. All the spring/damper elements represent the guidance rollers and thus the vertical travel is not constrained by them.

The main reason for the non-detailed description of the sledge model is the fact, that for the simulation the motion of the sledge will be completely determined of the measured motion of the real sledge. This approach has the advantage that all disturbances, which occur at the real world MULTI test system, can be investigated with the simulation. In addition, the very stiff connection of the sledge to the guidance is circumvented, and thus not every small unevenness has to be re-modeled for the simulation. The main disadvantage by this approach is that any effect of the damping motion to the sledge is not simulated. The feedback to the sledge by the damping motion has to be investigated in a separate simulation. The resulting dynamic consists of the mounting frame plus cabin, and the two damping actuators underneath the mounting frame forks, with three DOF. The basic separation of the model is shown in Figure 4.

The control output y of the model is chosen according to the definition of the ride comfort standard as the center of the cabin floor P_0 . Because the ride quality standard only punishes translational acceleration around the cabin floor, this is also the obvious choice as control output

$$y = h(q^b(t), u(t)) = \begin{bmatrix} a_{xc}(t) \\ a_{yc}(t) \\ a_{zc}(t) \end{bmatrix}. \quad (4)$$

Reduced Linear Model The linearization of the reduced model, thus the model without sledge and only three DOFs, is given by

$$M_{lin} \Delta \ddot{q}(t) = -K_{lin} \Delta q(t) - D_{lin} \Delta \dot{q}(t) + B u(t) \quad (5)$$

where the stiffness matrix K_{lin} and damping matrix D_{lin} are approximated by

$$\begin{aligned} K_{\text{lin}} &\approx \text{diag}(c_\alpha, c_\beta, c_\gamma) \in \mathbb{R}^{3 \times 3}, \\ D_{\text{lin}} &= \text{diag}(d_\alpha, d_\beta, d_\gamma) \in \mathbb{R}^{3 \times 3}, \end{aligned} \quad (6)$$

and the linear coordinates $\Delta q(t) = [\Delta\alpha_b, \Delta\beta_b, \Delta\gamma_b]^\top \in \mathbb{R}^3$ and $\Delta q(0) = \mathbf{0}$, $\Delta \dot{q}(0) = \mathbf{0}$. The stiffness matrix K_{lin} (6) ignores off-diagonal terms, which depend on the gravitational acceleration. These elements are small in comparison to the rotatory stiffness. The constant linear mass matrix $M_{\text{lin}} \in \mathbb{R}^{3 \times 3}$ contains the inertia and mass of the linear system. The input matrix $B_{\text{lin}} \in \mathbb{R}^{3 \times 2}$, which contains the levers of the forces f_1 and f_2 to the bearing at B_s . The linear model (5) was used for the parameter identification.

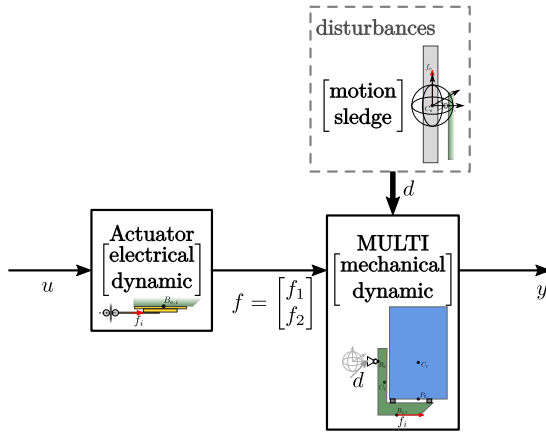


Fig. 4. Separation of the model in disturbance and cabin dynamic, including the actuator dynamics.

3.2 Electrical Dynamic

The electrical part of the model consists of the two linear motors used for vibration damping. Their dynamic equations given here can also be used as a non-distributed approximation of the actual propulsion of the PTS.

The electric equations of the linear motor are derived by transforming the rotational equations of the permanent magnet synchronous motor to a linear Permanent Magnet Linear Synchronous Motor (PMLSM), see e.g. Krishnan (2010), using the transformation

$$\omega_r = 2\pi \cdot f_r \quad (7)$$

from the electrical angular frequency ω_r and the electric frequency f_r . The dynamic model of the two-phased PMLSM in the rotor dq-frame is given by

$$\begin{aligned} u_{qs}^r &= R_s i_{qs}^r + L_{dq} \dot{i}_{qs}^r + \omega_r L_{dq} i_{ds}^r + \lambda_{af} \omega_r \\ u_{ds}^r &= R_s i_{ds}^r + L_{dq} \dot{i}_{ds}^r - \omega_r L_{dq} i_{qs}^r, \end{aligned} \quad (8)$$

where the voltages u_{qs}^r and u_{ds}^r are set by the current controller, the dynamic state of the motor model are the phase currents i_{qs}^r and i_{ds}^r . The phase inductance $L_q = L_d = L_{dq}$ are the same, because the magnets of the motor are surface mounted. The rest of the parameters are depicted in Table 1. Design of the current controller is not part of this paper and it assumed to be sufficiently fast.

The electrical velocity of the linear motor can be expressed using the pole pitch τ and (7) as

$$v_r = 2 \cdot \tau \cdot f_r = \frac{\tau}{\pi} \omega_r. \quad (9)$$

The electromagnetic force of a single actuator is therefore

$$f = \frac{3}{2} \frac{\pi}{\tau} \frac{Z_p}{2} \lambda_{af} i_{qs}^r, \quad (10)$$

using the substitution (9) and the relation between mechanical and rotor velocity $v_{\text{in}} = \frac{Z_p}{2} v_r$. The first actuator applies its force in the negative y -plane and the second in the positive, thus in the non-visible back of Figure 1. Force (10) is the force of a single actuator, which is duplicated for the second.

4. PARAMETER IDENTIFICATION

The underlying assumption of the model is that the three natural frequencies can be described by concentrated parameters at the bearing B_s between sledge and mounting frame. Therefore, the three pairs of spring/damper coefficients are determined using gray box estimation with the linear model (5). The identification is done in the frequency domain with a square error between measured and modelled frequency response. In addition, the natural frequencies are specified as points to be met. The measurements for the identification were performed using the two damping actuators and a stepped sine wave signal, with the frequencies from 1 to 30Hz in 0.5 Hz steps and orthogonal correlation analysis, see Isermann and Münchhof (2011). The presented identification was performed separately for each motor, thus one motor is turned off, while the other motor is used to excite the system using the sine wave signal. The resulting transfer function is plotted in Figure 5 for both inputs, thus from f_1 and f_2 , to the acceleration in y -direction at the cabin floor. It is clearly visible, that the main behavior of the system is well captured. The identified stiffness and damping coefficients are given in Table 1.

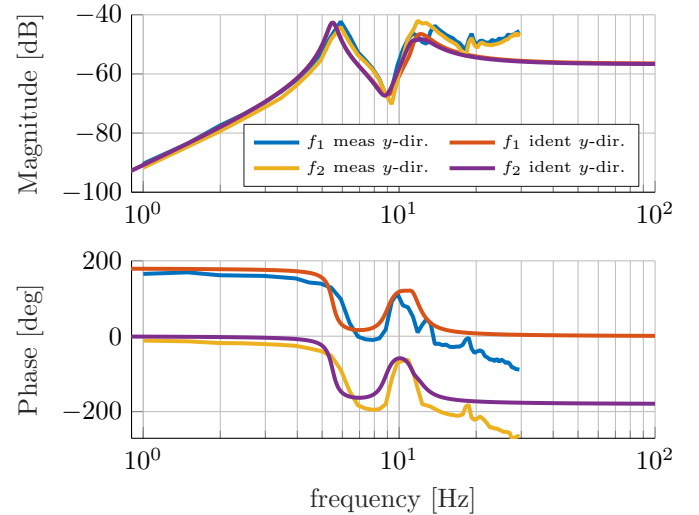


Fig. 5. Stepped sine-wave identification from the inputs f_1 and f_2 to the acceleration at the cabin floor in y -direction. Measured and identified transfer function.

5. SIMULATION

The non-linear model (3) is simulated with the parameters from Table 1. The input signal is the stepped sine wave

Table 1. Parameter of the reduced model and damping actuators.

Description	Parameter	Value
Mechanical		
<i>Position vector</i>		
$P_0 \rightarrow C_{bc}$	$r_{C_{bc}}^{P_0}$	$[-0.245 \ 0 \ -0.016]^T \text{ m}$
$B_s \rightarrow B_{e1,2}$	$r_{B_{e1,2}}^{B_s}$	$[0.611 \pm 0.538 \ -1.332]^T \text{ m}$
$B_s \rightarrow C_{bc}$	$r_{C_{bc}}^{B_s}$	$[0.670 \ 0 \ -0.916]^T \text{ m}$
$C_{e1,2} \rightarrow E_{s1,2}$	$r_{E_{s1,2}}^{C_{e1,2}}$	$[0.236 \ 0 \ 0.037]^T \text{ m}$
$S_{e1,2} \rightarrow C_{e1,2}$	$r_{C_{e1,2}}^{S_{e1,2}}$	$[0.504 \pm 0.039 \ 0.030]^T \text{ m}$
$C_{eu1,2} \rightarrow B_{e1,2}$	$r_{B_{e1,2}}^{C_{eu1,2}}$	$[0 \ 0 \ 0.016]^T \text{ m}$
$E_{b1,2} \rightarrow C_{eu1,2}$	$r_{C_{eu1,2}}^{E_{b1,2}}$	$[0 \ 0 \ 0.015]^T \text{ m}$
$B_s \rightarrow C_s$	$r_{C_s}^{B_s}$	$[-0.11 \ 0 \ 0]^T \text{ m}$
$\mathcal{O} \rightarrow C_s$	$r_{C_s}^{\mathcal{O}}$	$[0.19 \ 0 \ 0]^T \text{ m}$
$\mathcal{O} \rightarrow B_s$	$r_{B_s}^{\mathcal{O}}$	$[0.3 \ 0 \ 0]^T \text{ m}$
<i>Stiffness ...</i>		
... around x -axis	c_{α_b}	$8.446 \cdot 10^5 \text{ N/m}$
... around y -axis	c_{β_b}	$3.100 \cdot 10^6 \text{ N/m}$
... around z -axis	c_{γ_b}	$7.319 \cdot 10^5 \text{ N/m}$
<i>Damping coefficient ...</i>		
... around x -axis	d_{α_b}	$2.183 \cdot 10^3 \text{ N s/m}$
... around y -axis	d_{β_b}	$4.182 \cdot 10^3 \text{ N s/m}$
... around z -axis	d_{γ_b}	$2.032 \cdot 10^3 \text{ N s/m}$
Gravitation	g	9.81 m/s^2
<i>Mass</i>		
Mounting frame + cabin	m_{bc}	345 kg
Mass active part	m_{el}	28.5 kg
Mass passive part	m_{eu}	4.68 kg
<i>Inertia (main diagonal)</i>		
Mounting frame + cabin	$I_{bc}^{C_{bc}}$	$[137.07 \ 135.77 \ 131.98]^T \text{ kg} \cdot \text{m}^2$
Active part actuator	$I_{el}^{C_{el}}$	$[0.144 \ 0.919 \ 1.051]^T \text{ kg} \cdot \text{m}^2$
Passive part actuator	$I_{eu}^{C_{eu}}$	$[0.028 \ 0.257 \ 0.286]^T \text{ kg} \cdot \text{m}^2$
Motor electric parameters		
Induction	L_{dq}	0.030 H
Stator resistance	R_s	3.8 Ω
Armature flux linkage	λ_{af}	1.429 V \cdot s
Pole pitch	τ	0.024 m
Pole pairs	Z_p	2

used for the identification. The Figure 6 displays the acceleration at the center of the cabin floor P_0 at 9.5 and 10 Hz. The simulated acceleration is compared to the measured acceleration. Only the first damping actuator is used to excite the system, thus the second is kept at zero. The amplitude of the sine wave was set to 400 N. While it is visible that the real system contains an overlaying high-frequent dynamic not modeled with (3), visible for example at 93 s in the Figure 6, the excitation around 9.5 Hz is clearly modeled well. The short simulation excerpt shows that the dominant frequencies dominant are mapped by the model.

6. CONCLUSION

An MBS of the novel rope-free PTS was presented in this paper. The main aim of the model is the active vibration damping inside the cabin of the PTS, therefore the active damping components attached to the mounting frame are also included in the model with closed kinematic chain. The dynamic parameters for the three spring/damper pairs at the bearing were determined by gray-box identification. The identification uses data obtained using stepped sine wave measurements, which were performed at the MULTI test system at the thyssenkrupp test tower in Rottweil, Germany, showing good results. While the propulsion system of the PTS was not part of the model, the linear motor equations presented can be used as a first approximation. The model forms a good

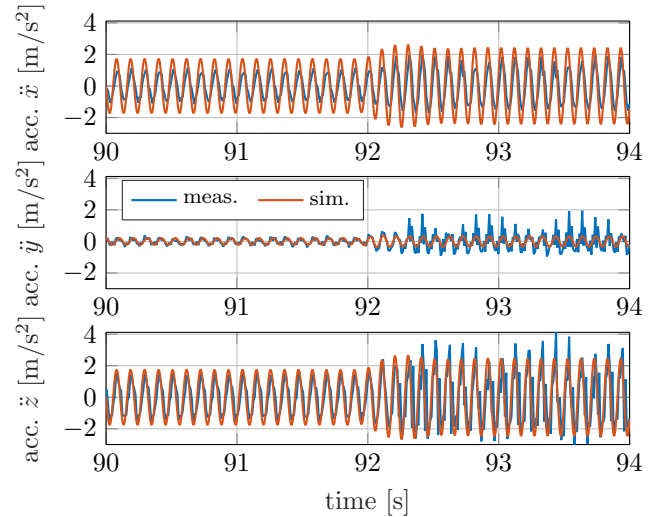


Fig. 6. Comparison between measured and simulation acceleration at the cabin floor P_0 .

basis for the active cabin vibration damping on the actual MULTI test system in Rottweil.

ACKNOWLEDGEMENTS

The authors would like to thank thyssenkrupp Elevator AG, Rottweil, Germany, for their ongoing support.

REFERENCES

- Appunn, R., Frantzheld, J., Jetter, M., and Löser, F. (2018). MULTI® - rope-less elevator demonstrator at test tower Rottweil. *Transportation Systems and Technology*, 4(3), 80–89. doi:10.17816/transsyst20184380-89.
- Bottasso, C.L. (ed.) (2009). *Multibody dynamics*, volume 12 of *Computational methods in applied sciences*. Springer, Politecnico di Milano, Italy. doi:10.1007/978-1-4020-8829-2.
- DE2002081 (A1). Karl Kudermann. (1970). Elektrischer Antrieb fuer Lastenfoerderer.
- Heinrich, K. and Kretzschmar, R. (1989). *Transrapid MagLev system*. Hestra-Verlag.
- Isermann, R. and Münchhof, M. (2011). *Identification of Dynamic Systems: An Introduction with Applications*. Springer-Verlag, Berlin Heidelberg.
- ISO18738-1:2012 (2012). Measurement of ride quality - Part 1: Lifts (elevators).
- ISO2631-1:1997 (1997). Mechanical vibration and shock - Evaluation of human exposure to whole-body vibration - Part 1: General requirements.
- Krishnan, R. (2010). *Permanent magnet synchronous and brushless DC motor drives*. CRC Press, Boca Raton Fla. u.a.
- Missler, J., Ehrl, T., Meier, B., Kaczmarczyk, S., and Sawodny, O. (2016). Modelling of a rope-free passenger transportation system for active cabin vibration damping. *6th Lift and Escalator Symposium*, 2016.
- VDI2057 (2015). Human exposure to mechanical vibrations whole-body vibration.